Stem Cell Reports
Resource
ISSCR
OPEN ACCESS

A Simplified, Fully Defined Differentiation Scheme for Producing Blood-Brain Barrier Endothelial Cells from Human iPSCs

Emma H. Neal,[1] Nicholas A. Marinelli,[2] Yajuan Shi,[1] P. Mason McClatchey,[3] Kylie M. Balotin,[4] Dalton R. Gullett,[1] Kameron A. Hagerla,[1] Aaron B. Bowman,[5] Kevin C. Ess,[6,7] John P. Wikswo,[3,4,8,9] and Ethan S. Lippmann[1,2,4,*]

[1]Department of Chemical and Biomolecular Engineering, Vanderbilt University, Nashville, TN, USA
[2]Chemical and Physical Biology Program, Vanderbilt University, Nashville, TN, USA
[3]Department of Molecular Physiology and Biophysics, Vanderbilt University, Nashville, TN, USA
[4]Department of Biomedical Engineering, Vanderbilt University, Nashville, TN, USA
[5]School of Health Sciences, Purdue University, West Lafayette, IN, USA
[6]Department of Pediatrics, Vanderbilt University Medical Center, Nashville, TN, USA
[7]Department of Neurology, Vanderbilt University Medical Center, Nashville, TN, USA
[8]Department of Physics and Astronomy, Vanderbilt University, Nashville, TN, USA
[9]Vanderbilt Institute for Integrative Biosystems Research and Education, Vanderbilt University, Nashville, TN, USA
*Correspondence: ethan.s.lippmann@vanderbilt.edu
https://doi.org/10.1016/j.stemcr.2019.05.008

SUMMARY

Human induced pluripotent stem cell (iPSC)-derived developmental lineages are key tools for *in vitro* mechanistic interrogations, drug discovery, and disease modeling. iPSCs have previously been differentiated to endothelial cells with blood-brain barrier (BBB) properties, as defined by high transendothelial electrical resistance (TEER), low passive permeability, and active transporter functions. Typical protocols use undefined components, which impart unacceptable variability on the differentiation process. We demonstrate that replacement of serum with fully defined components, from common medium supplements to a simple mixture of insulin, transferrin, and selenium, yields BBB endothelium with TEER in the range of 2,000–8,000 $\Omega \times cm^2$ across multiple iPSC lines, with appropriate marker expression and active transporters. The use of a fully defined medium vastly improves the consistency of differentiation, and co-culture of BBB endothelium with iPSC-derived astrocytes produces a robust *in vitro* neurovascular model. This defined differentiation scheme should broadly enable the use of human BBB endothelium for diverse applications.

INTRODUCTION

The blood-brain barrier (BBB) is composed of brain microvascular endothelial cells (BMECs), which strictly maintain CNS homeostasis by regulating material exchange between the bloodstream and parenchyma (Obermeier et al., 2013). Disruption of the BBB is strongly implicated in many neurodegenerative diseases (Zlokovic, 2008), and its functions are also influenced by peripheral conditions that can reduce its fidelity and result in CNS damage (Huber et al., 2001). Conversely, an intact BBB prevents efficient delivery of therapeutics to the CNS. Thus, a better understanding of BBB properties is vital for the treatment of CNS disorders.

In vitro BBB models are often used to study mechanisms of neurovascular regulation and dysfunction during disease, and also can serve as a tool for high-throughput screening of BBB-permeant compounds. Historically, most BBB models have been constructed from primary animal sources, but it is well-recognized that a human model would be preferred owing to general species differences (Helms et al., 2016; Syvänen et al., 2009). However, until recently, *in vitro* human BBB models were limited to either primary (Bernas et al., 2010) or immortalized BMECs (Weksler et al., 2005), whereas each source has downsides in terms of yield and barrier fidelity.

In 2012, human pluripotent stem cells (hPSCs) were successfully differentiated to BMECs, as determined by increased transendothelial electrical resistance (TEER) ($\sim$850 $\Omega \times cm^2$), representative permeability to a cohort of small molecules, and active efflux transporter function (Lippmann et al., 2012). The addition of retinoic acid (RA) during the differentiation process further enhanced passive barrier function (TEER $\sim$3,000 $\Omega \times cm^2$) (Lippmann et al., 2014a). These BMECs have been used for mechanistic interrogations (Stebbins et al., 2017) and are effective for modeling BBB-specific disease mechanisms (Vatine et al., 2017). However, limitations still exist in the differentiation process. TEER has been estimated *in vivo* up to 8,000 $\Omega \times cm^2$ based on radioactive ion permeabilities (Smith and Rapoport, 1986), and although this value may not be the absolute upper limit in humans, hPSC-derived BMECs in monoculture typically exhibit about half of this TEER threshold (Appelt-Menzel et al., 2017; Hollmann et al., 2017; Vatine et al., 2017). Moreover, BMEC differentiation generally relies on the use of serum-containing medium, which limits consistency and reliability of the final purified population. Despite

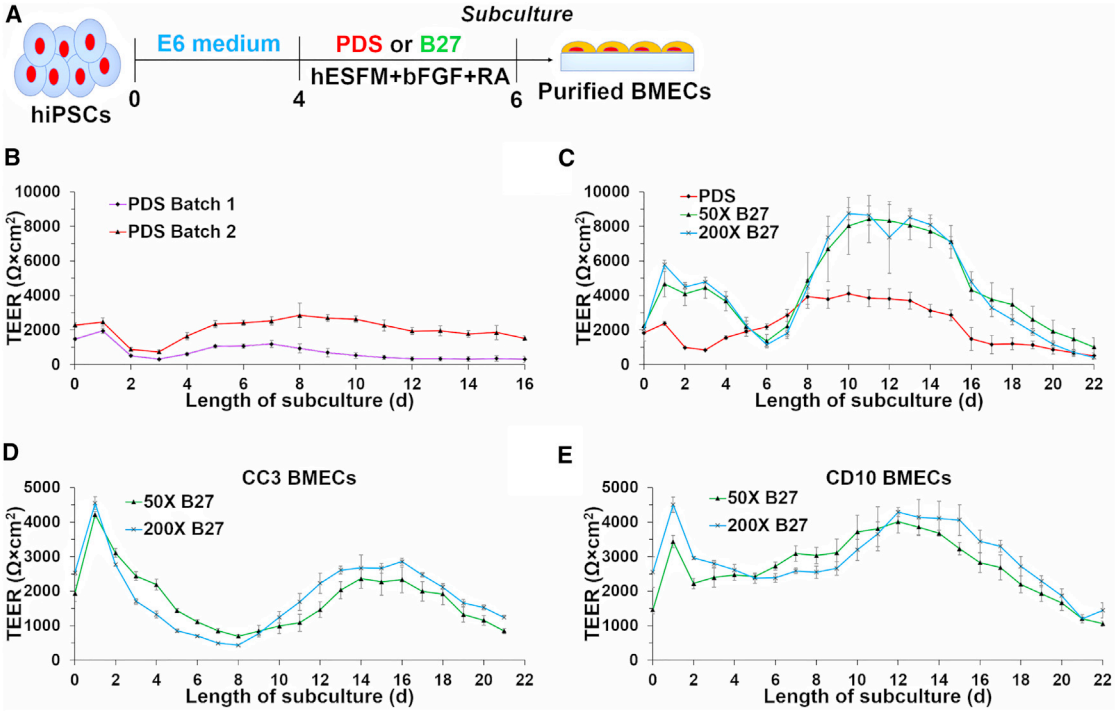

Figure 1. Exclusion of Serum during the Differentiation of iPSCs to BMECs Yields Robust Passive Barrier Properties

(A) Differentiation scheme, including media variations and timing.

(B) iPSCs differentiated concurrently with different batches of serum exhibit varying passive barrier phenotype as assessed by TEER.

(C) iPSCs were differentiated concurrently using PDS, 50× diluted B27, or 200× diluted B27.

(D and E) CC3 BMECs (D) and CD10 BMECs (E) produce equivalent TEER profiles at 50× and 200× B27 dilutions. Trends were confirmed across biological N = 3.

advancements in standardization of the differentiation process (Hollmann et al., 2017; Wilson et al., 2015), more work is needed to achieve optimum results.

Here, we detail an unexpected improvement to the BBB differentiation procedure when transitioning to serum-free methods. By replacing the serum component of the differentiation medium with fully defined factors, we can consistently achieve TEER maxima of 2,000–8,000 Ω × cm^2 in BMEC monocultures across multiple induced pluripotent stem cell (iPSC) lines, with expected marker expression and transporter activity. The defined procedure also consistently generated a barrier phenotype in BMECs derived from several disease-specific lines that was equal or better than BMECs derived in serum. Moreover, the exclusion of serum significantly enhanced the responsiveness of BMECs to co-culture with astrocytes, with maximum TEER values reproducibly exceeding 9,000–10,500 Ω × cm^2. These advances in differentiation technique are expected to have a positive impact toward using iPSC-derived BMECs to model age- and disease-related declines in BBB function.

RESULTS

Serum-free Medium Yields iPSC-Derived BMECs with Enhanced TEER

The confounding influence of serum and serum-derived proteins on hPSC differentiation has been well-documented (Mannello and Tonti, 2007), and the development of fully defined differentiation protocols is thus recognized as an important step for standardizing hPSC research applications. As such, we sought to replace the serum in our BBB differentiation process with more defined components. Our most recent differentiation scheme seeds iPSCs at a defined density, followed by differentiation for 4 days in fully defined E6 medium (Hollmann et al., 2017), then 2 days in a basal endothelial medium supplemented with platelet-poor plasma-derived serum (PDS), basic fibroblast growth factor (bFGF), and RA. BMECs are subsequently purified for phenotypic analyses (Figure 1A). A direct comparison of two different lots of PDS showed marked differences in the passive barrier properties of the final BMEC population derived from CC3 iPSCs (Figure 1B), a line that has been used

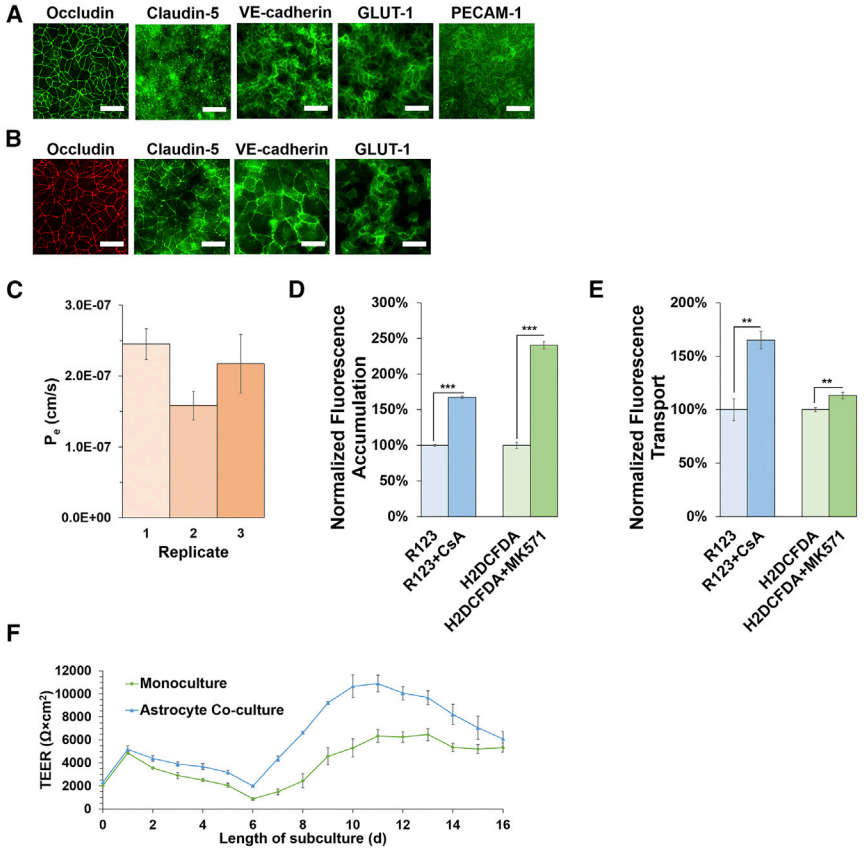

Figure 2. Further Evaluation of Passive and Active Barrier Functions of BMECs Differentiated under Serum-free Conditions

(A) Immunocytochemical detection of occludin, claudin-5, VE-cadherin, GLUT-1, and PECAM-1 on day 6 of differentiation. Scale bars, 50 μm.

(B) Immunocytochemical detection of occludin, claudin-5, VE-cadherin, and GLUT1 48 h following purification. Scale bars, 50 μm.

(C) Effective permeability of sodium fluorescein for biological N = 3. Data are reported as mean ± SD from technical triplicates.

(D) Intracellular fluorescence accumulation was measured in cells incubated with P-glycoprotein and MRP substrates and inhibitors. All values are reported as mean ± SD from technical triplicates. Statistical significance was determined using Student's unpaired t test (***$p < 0.001$). Trends were confirmed across biological N = 3.

(E) Apical to basolateral flux of rhodamine-123 (R123) and H_2DCFDA in the presence or absence of cyclosporin A (CsA) and MK-571, respectively. Data are reported as normalized mean ± SD from technical triplicates. Statistical significance was determined using Student's unpaired t test (**$p < 0.01$). Trends were confirmed across biological N = 3.

(F) TEER measurements in CC3-derived BMECs co-cultured with CC3-derived astrocytes. Trends were confirmed across biological N = 3.

previously with good success (Hollmann et al., 2017). Specifically, 44% of BMEC differentiations failed to reach TEER exceeding 1,000 Ω × cm^2 using a single lot of PDS (N = 9 biological replicates; data not shown), while differentiations conducted using a second lot of PDS consistently reached TEER maxima in excess of 2,000 Ω × cm^2. We decided, therefore, to replace PDS with B27, a common serum alternative in neural cultures (Brewer et al., 1993), tested at either 50× (the manufacturer's recommendation) or 200× dilution (Figure 1A). Surprisingly, while a pre-qualified batch of PDS could produce BMECs with the expected maximum TEER of ~4,000 Ω × cm^2, B27 supplementations produced maximum TEER above 8,000 Ω × cm^2 (8,734 ± 349 Ω × cm^2 in 200× B27) (Figure 1C). CC3-derived BMECs (Figure 1D) and CD10-derived BMECs (Figure 1E), female and male control lines (Kumar et al., 2014; Tidball et al., 2016), respectively, consistently achieved maximum TEER values in excess of 3,000 Ω × cm^2 across more than 10 independent CC3 differentiations and in excess of 2,000 Ω × cm^2 across 4 independent CD10 differentiations.

Additional Characterization of iPSC-Derived BMEC Phenotype under Serum-free Conditions

To follow up on the TEER measurements, we assayed other properties of iPSC-derived BMECs under serum-free conditions. Immediately before purification, BMECs expressed occludin, claudin-5, VE-cadherin, GLUT-1, and PECAM-1, indicating acquisition of a BBB phenotype as typically seen in PDS (Figure 2A). BMECs were again evaluated 48 h after purification, and expressed occludin, claudin-5, VE-cadherin, and GLUT-1 (Figure 2B). Paracellular permeability was assessed using sodium fluorescein, and all replicates had effective permeabilities less than 2.5 × 10^{-7} cm/s, similar to BMECs differentiated in PDS (Hollmann et al., 2017) (Figure 2C). Collectively, these results indicate that replacement of serum with B27 during differentiation produces BMECs with robust passive barrier properties, with the added benefit of eliminating reliance on an undefined material with substantial lot-to-lot variability. BMECs were next evaluated for efflux activity of P-glycoprotein and multidrug resistance protein (MRP) transporters. P-glycoprotein activity was assessed by measuring fluorescence accumulation in purified BMECs

incubated either with rhodamine-123, a fluorescent P-glycoprotein substrate, or rhodamine-123 containing cyclosporin A, a P-glycoprotein inhibitor. BMECs incubated with inhibitor showed a significant increase in fluorescence accumulation, indicating active P-glycoprotein function (Figure 2D). Similarly, purified BMECs were incubated with H_2DCFDA with or without MK-571, an inhibitor of the MRP family, and showed increased fluorescence accumulation compared with control cells, indicating MRP activity (Figure 2D). Directionality of P-glycoprotein and MRP transport was assessed by measuring the transport of fluorescent substrate across the monolayer of purified BMECs cultured on Transwell filters. Increased apical to basolateral substrate transport (mimicking blood to brain) was observed on BMEC treatment with cyclosporin A and MK-571, indicating expected P-glycoprotein and MRP polarization (Figure 2E). Last, we co-cultured BMECs with astrocytes, an important constituent of the neurovascular unit previously reported to improve BBB functionality (Canfield et al., 2017), and re-evaluated TEER. Interestingly, BMECs co-cultured with astrocytes reach higher TEER by day 11 of subculture than BMECs in monoculture, exceeding 9,000 $\Omega \times cm^2$ in biological replicates (Figure 2F). These results indicate BMEC responsiveness to astrocytic cues, and the overall dataset validates the BMEC phenotype in serum-free conditions.

Serum-free Medium Yields BMECs with Adequate Passive Barrier Function from Disease Lines

Recently, it was reported that iPSC-derived BMECs from Huntington's disease (HD) patients exhibit defunct barrier properties that correlate with the severity of the CAG repeat, including an inability to form any physical barrier as measured by TEER and compromised P-glycoprotein activity (Lim et al., 2017). Our group had experienced similar unreported difficulties when differentiating patient-derived HD and tuberous sclerosis complex (TSC) iPSCs to BMECs using serum-based methods. Given the striking increase in TEER and improved consistency achieved when differentiating control iPSCs using serum-free medium, we investigated whether this method could rescue the phenotype in disease lines. HD70-2 iPSCs, harboring a 70 CAG repeat (Tidball et al., 2016), and TSP8-15, harboring a nonsense *TSC2* mutation (characterization provided in Figure S1), were differentiated using either B27 or PDS, and TEER of resultant BMECs from both conditions was assessed (Figures 3A and 3B, respectively). Notably, for both disease lines, TEER was elevated in BMECs differentiated using B27 rather than PDS across multiple biological replicates (Figure 3C).

Given the previous challenges observed in differentiating HD lines to BMECs, we further evaluated the BBB phenotype in HD70-2-derived BMECs. Purified HD70-2-derived BMECs show clear expression of claudin-5, occludin, VE-cadherin, and GLUT-1, as expected for brain endothelium (Figure 3D). We subsequently quantified the fidelity of claudin-5 and occludin expression in HD70-2-derived BMECs and CC3-derived BMECs by normalizing the areal expression of the junction proteins to cell count (Figure 3E). Although no differences in occludin localization were observed, HD70-2-derived BMECs expressed significantly less claudin-5 per cell than CC3-derived BMECs. HD70-2-derived BMECs also displayed active P-glycoprotein function as demonstrated by a significant increase in fluorescence accumulation in cells treated with inhibitor (Figure 3F). Thus, the HD70-2 iPSC line can successfully produce BMECs.

Fully Defined Medium with Minimal Components Can Produce High-Fidelity BMECs

To further simplify the differentiation scheme, we sought to identify specific components of B27 that were essential to a successful BMEC differentiation. To this end, iPSCs were differentiated using N2, a chemically defined, serum-free supplement with known component concentrations (Bottenstein, 1985), in place of B27. The resultant BMECs consistently achieved maximum TEER values greater than 2,500 $\Omega \times cm^2$ across seven biological replicates, indicating the presence of an intact endothelial monolayer, and suggesting a successful differentiation outcome (Figure 4A). We further noted that selenium, insulin, and transferrin were among the conserved components between N2 and B27 and are also core components of E6 medium (Lippmann et al., 2014b). We therefore posited that basal endothelium medium supplemented with insulin, transferrin, and selenium (referred to as ITS) might be suitable for BMEC derivation. This hypothesis was supported by the resultant BMEC monolayers differentiated in ITS also achieving maximum TEER values greater than 2,500 $\Omega \times cm^2$ across seven biological replicates (Figure 4A). The long-term stability of CC3-derived BMECs was tracked and found to be similar to that of BMECs differentiated using B27 and N2 (Figure 4B). The ITS scheme was further tested in CD10-derived BMECs to ensure the method was applicable across iPSC lines, and the long-term TEER stability was similar to CC3-derived BMECs (Figure 4C). VE-cadherin, occludin, claudin-5, and GLUT-1 were also uniformly expressed in cells differentiated in ITS (Figure 4D). In addition, cells differentiated in ITS displayed restricted paracellular permeability to sodium fluorescein (Figure 4E) and active P-glycoprotein and MRP function (Figure 4F), indicating acquisition of the BMEC phenotype. Thus, the undefined, serum-based differentiation procedure used to previously produce BMECs from iPSCs can ultimately be reduced to three fully defined media additives without compromising passive barrier integrity.

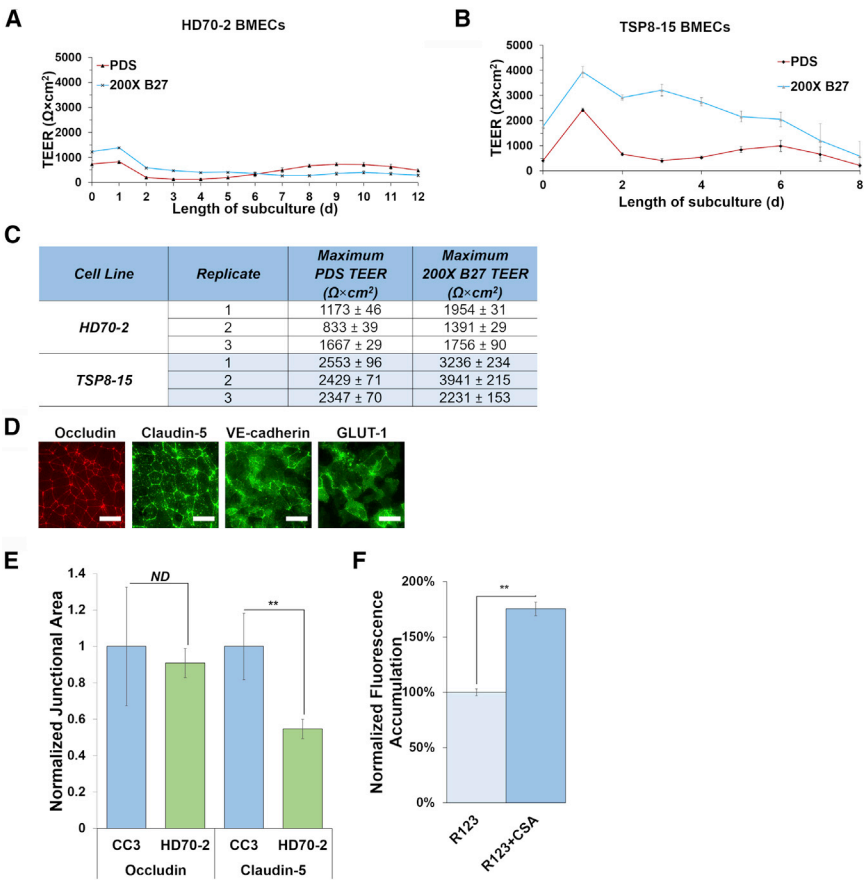

Cell Line	Replicate	Maximum PDS TEER (Ω×cm²)	Maximum 200X B27 TEER (Ω×cm²)
HD70-2	1	1173 ± 46	1954 ± 31
	2	833 ± 39	1391 ± 29
	3	1667 ± 29	1756 ± 90
TSP8-15	1	2553 ± 96	3236 ± 234
	2	2429 ± 71	3941 ± 215
	3	2347 ± 70	2231 ± 153

Figure 3. Serum-free Differentiation Improves BMEC Fidelity in iPSC Lines Harboring Known Disease Mutations

(A and B) HD70-2 (A) and TSP8-15 (B) iPSCs were differentiated to purified BMECs using either PDS or 200× diluted B27, and TEER was measured approximately every 24 h after purification.

(C) Differentiations were replicated for an additional biological N = 2 to examine reproducibility.

(D) Immunocytochemical detection of occludin, claudin-5, VE-cadherin, and GLUT-1 in purified HD70-2 BMECs. Scale bars, 50 μm.

(E) Normalized junctional area for claudin-5 and occludin in HD70-2-derived BMECs and CC3-derived BMECs was calculated across a minimum of three fields per marker. Statistical significance was determined using Student's unpaired t test (**p < 0.01).

(F) Intracellular fluorescence accumulation was measured in purified HD70-2 BMECs incubated with rhodamine-123 (R123) in the presence or absence of the inhibitor cyclosporin A (CsA). All values are reported as mean ± SD from technical triplicates. Statistical significance was determined using Student's unpaired t test (***p < 0.001). Trends were confirmed across biological N = 3.

DISCUSSION

The variability of differentiation outcomes resulting from batch-to-batch changes in serum composition and quality constitutes a significant hurdle in the use of iPSCs for research and prospective regenerative medicine applications. In this study, we sought to address this issue in the context of BMEC differentiation through the replacement of serum with more defined supplements. This advancement ultimately mitigates procedural variability, thereby providing researchers with more reliable and robust iPSC-derived BMECs to interrogate neurovascular function.

The present study was motivated by our initial observations that different lots of PDS (the serum component in our differentiation medium) produced BMECs of dramatically different quality and in some cases resulted in completely failed differentiations. Qian et al. (2017) published a fully defined differentiation procedure in which iPSCs were differentiated to BMECs as a homogeneous population through a mesoderm intermediate, whereas all previous BMEC differentiation procedures have relied on a co-differentiation approach in which the resultant BMECs must be purified from the mixed neural/endothelial cultures. Despite these differences in approach, we suspected that the use of fully defined components may translate to the co-differentiation system used by most researchers. Indeed, in our first experiments, BMECs differentiated using B27 yielded maximum TEER in excess of 8,000 Ω × cm^2 in monoculture. We note that this female iPSC line (CC3) did not always produce BMECs with TEER up to *in vivo* levels under these defined conditions, nor did the male control line CD10. Indeed, TEER often fell within a range of 2,000–5,000 Ω × cm^2. We attribute a significant portion of this variability to differences in user skill, noting that subtle differences in culture techniques during iPSC maintenance and differentiation can result in noticeably different TEER profiles and maxima. In addition, we have observed that BMEC performance, particularly at later timepoints in subculture, appears to be influenced by conditioning of the medium by the BMECs. We speculate that metabolic differences between iPSC lines and passages may influence this conditioning and thereby contribute to the observed TEER variability. Regardless, both iPSC lines consistently produced BMECs

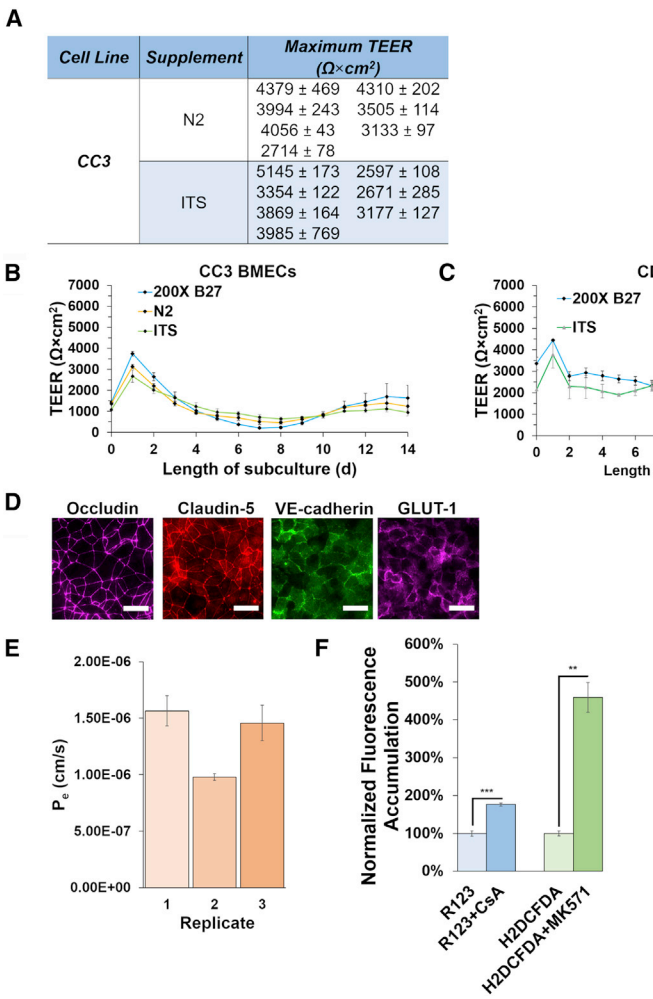

Figure 4. Fully Defined Differentiation Medium Produces BMECs

(A) iPSCs were differentiated to BMECs using either 1× N2 supplement or a custom cocktail of insulin, transferrin, and selenium (ITS). TEER was measured approximately every 24 h after purification. Biological N = 7 per condition.

(B and C) The long-term stability of CC3-derived BMECs (B) and CD10-derived BMECs (C) differentiated using 200× diluted B27, 1× N2 (CC3 only), or ITS was tracked via TEER measurements. Biological N = 3 per condition per line.

(D) Immunocytochemical detection of occludin, claudin-5, VE-cadherin, and GLUT-1 in purified CC3 BMECs differentiated in ITS. Scale bars, 50 μm.

(E) Effective permeability of sodium fluorescein across biological N = 3 for CC3-derived BMECs differentiated using ITS. Data are reported as mean ± SD from technical triplicates.

(F) Intracellular fluorescence accumulation was measured in CC3-derived BMECs differentiated using ITS incubated with P-glycoprotein and MRP substrates and inhibitors. All values are reported as mean ± SD from technical triplicates. Statistical significance was determined using Student's unpaired t test (**p < 0.01, ***p < 0.001). Trends were confirmed across biological N = 3.

with maximum TEER above 2,000 Ω × cm^2, with no differentiations failing to reach TEER above 1,000 Ω × cm^2 across a total of 14 independent biological replicates and multiple users. Such maximum values are in line with values achieved using previously established methods (Lippmann et al., 2014a; Wilson et al., 2015), with the benefit of utmost reproducibility. In addition, co-culture with astrocytes elevated TEER further, exceeding 9,000 Ω × cm^2 across multiple biological replicates. For reference, we previously showed that BMECs differentiated with serum and co-cultured with astrocytes in serum-containing medium exhibited maximum TEER of ~5,000 Ω × cm^2 (Hollmann et al., 2017). To our knowledge, this TEER value was previously unattainable using serum-based procedures. We suspect two possibilities for this enhanced response to astrocyte co-culture. First, the removal of serum during differentiation may alter BMEC properties and make the cells more responsive to soluble cues from astrocytes. Second, given that serum was previously present during co-culture, its absence may yield healthier astrocytes, which then communicate more effectively with BMECs. We intend to follow up on this outcome; but, regardless, our results indicate that the serum-free system may have substantial usefulness for assessing mechanisms of neurovascular crosstalk.

Following rigorous assessments of TEER, BMECs differentiated using B27 were evaluated for other characteristic BBB properties. The effective permeability of sodium fluorescein across the monolayer was on the order of 10^{-7} cm/s across three biological replicates, in line with previously published data by our group and others (Hollmann et al., 2017; Wilson et al., 2015). BMECs differentiated using B27 were shown to have active P-glycoprotein and MRPs as demonstrated by increases in fluorescent substrate accumulation and expected P-glycoprotein polarization. The VE-cadherin$^+$ BMECs also expressed expected BBB markers, including tight junction proteins and GLUT-1. These results further suggest that the substitution of serum with B27 in the differentiation procedure ultimately results in BMECs of equal fidelity to previously reported methods.

Next, we evaluated the performance of BMECs differentiated from two iPSC lines harboring mutations implicated in neurological/neurodegenerative disease. BBB dysfunction is associated with multiple neurodegenerative diseases and is increasingly being recognized as a potential therapeutic target in the treatment of such diseases (Banks, 2016; Zlokovic, 2008). Human iPSCs therefore present an unprecedented opportunity to model neurovascular function in health and disease, and to assess drug treatments *in vitro*. However, iPSC lines with disease-causing mutations are often more difficult to handle and differentiate, as mutations can impart features such as genomic instability (Tidball et al., 2016). These difficulties confound interpretation of experimental results as it is often unclear whether observed outcomes are a true feature of the disease in question or rather due to other factors, such as sensitivity to *in vitro* culture conditions unrelated to the disease phenotype. To address this issue, we differentiated iPSCs from patients with HD and TSC using both serum-based and B27-based procedures. For both sets of iPSCs, we routinely observed higher maximum TEER in BMECs differentiated using B27 compared with those using serum in three independent biological replicates. Furthermore, HD iPSC-derived BMECs differentiated in B27 were found to express key molecular markers of BBB phenotype, although claudin-5 expression had lower fidelity in HD iPSC-derived BMECs compared with control BMECs, and possessed active P-glycoprotein. These results contrast with a previous report where BMECs differentiated from an HD iPSC line with a similar CAG repeat could not form any appreciable barrier and had lower efflux activity relative to control BMECs (Lim et al., 2017). Our findings certainly do not invalidate either the previous observations or the proposed mechanism behind the barrier defects, especially since the HD lines in each study were not identical, but they do again caution that a failure to produce the appropriate BBB phenotype in a given cell line may not always reflect the disease being modeled. More broadly, the ability to create high-fidelity BMECs from disease lines should open new opportunities to investigate neurodegenerative diseases from a holistic neurovascular perspective.

Last, despite the advantages of B27 as a serum-free supplement, we were concerned that its composition is proprietary. BBB function can be influenced by different components that regulate diverse signaling pathways (Salvador et al., 2014); therefore, if the goal of an experiment is to dynamically investigate the influence of any one particular component on BBB function in real-time, it is desirable to precisely control the composition of the medium. We thus evaluated a chemically defined supplement (N2), as well as a defined mixture of insulin, transferrin, and selenium. Regardless of the supplement composition, resultant BMECs achieved passive barrier properties well above that considered to be a functional barrier (TEER above 500–1,000 $\Omega \times cm^2$) (Mantle et al., 2016). BMECs also displayed active P-glycoprotein and MRP function. We further note that, although we used Matrigel as the substrate for differentiation, it could be replaced with a fully defined substrate to further standardize this procedure. Overall, the use of fully defined medium represents a robust, reproducible, and cost-effective approach to investigating BBB physiology *in vitro* in both healthy and diseased states, thereby facilitating broader adoption of iPSC-derived BMEC models across the greater research community.

EXPERIMENTAL PROCEDURES

iPSC Differentiation to BMECs

iPSCs were seeded onto a Matrigel-coated plate in E8 medium containing 10 μM Y-27632 at a density of 15,800 cells/cm^2. Differentiation was initiated 24 h after seeding by switching medium to E6 medium. E6 medium was replenished every 24 h for 4 days. After 4 days, cells were switched to basal endothelial medium (hESFM) supplemented with bFGF and RA and either PDS, B27, N2, or ITS, depending on the experiment. Medium was not changed for 48 h. After 48 h, cells were collected and replated onto Transwell filters or cell culture plates coated with collagen IV and fibronectin. Twenty-four hours after replating, bFGF and RA were removed from the medium to induce barrier phenotype.

SUPPLEMENTAL INFORMATION

Supplemental Information can be found online at https://doi.org/10.1016/j.stemcr.2019.05.008.

AUTHOR CONTRIBUTIONS

Conceptualization, E.H.N. and E.S.L.; Methodology, E.H.N., A.B.B., and E.S.L.; Investigation, E.H.N., Y.S., N.A.M., P.M.McC., K.M.B., D.R.G., and K.A.H.; Writing – Original Draft, E.H.N. and E.S.L.; Writing – Review & Editing, E.H.N., A.B.B., K.C.E., J.P.W., and E.S.L.; Funding Acquisition, A.B.B., K.C.E., J.P.W., and E.S.L.; Supervision, E.S.L.; Project Administration, E.S.L.

ACKNOWLEDGMENTS

Funding for this work was graciously provided by the donors of Alzheimer's Disease Research, a program of the BrightFocus Foundation (grant A20170945 to E.S.L.), as well as a NARSAD Young Investigator Award from the Brain and Behavior Research Foundation (grant 25177 to E.S.L.), a Ben Barres Early Career Acceleration Award from the Chan Zuckerberg Initiative (grant 2018-191850 to E.S.L.), NSF grant 1706155 (to E.S.L.), and NIH grants R21 NS106510 (to E.S.L.), R01 NS078289 (to K.C.E.), R01 ES016931 (to A.B.B.), and UG3 TR002097 (to J.P.W., K.C.E., and A.B.B.). Additional funding was provided by Intelligence Advanced Research Projects Activity (IARPA) contract 2017-17081500003 (to J.P.W.) and Defense Threat Reduction Agency (DTRA) grant CBMXCELXL1-2-001 through Los Alamos National Laboratory Subcontract 468746 (to J.P.W.). E.H.N. is supported by a Graduate Research

Fellowship from the NSF (DGE-1445197). N.A.M. is supported by the Integrated Training in Engineering and Diabetes Program (T32 DK101003). K.M.B. is supported by the Training Program in Environmental Toxicology (T32 ES007028).

Received: October 8, 2018
Revised: May 9, 2019
Accepted: May 10, 2019
Published: June 11, 2019

REFERENCES

Appelt-Menzel, A., Cubukova, A., Günther, K., Edenhofer, F., Piontek, J., Krause, G., Stüber, T., Walles, H., Neuhaus, W., and Metzger, M. (2017). Establishment of a human blood-brain barrier co-culture model mimicking the neurovascular unit using induced pluri- and multipotent stem cells. Stem Cell Reports *8*, 894–906.

Banks, W.A. (2016). From blood-brain barrier to blood-brain interface: new opportunities for CNS drug delivery. Nat. Rev. Drug Discov. *15*, 275–292.

Bernas, M.J., Cardoso, F.L., Daley, S.K., Weinand, M.E., Campos, A.R., Ferreira, A.J.G., Hoying, J.B., Witte, M.H., Brites, D., Persidsky, Y., et al. (2010). Establishment of primary cultures of human brain microvascular endothelial cells to provide an in vitro cellular model of the blood-brain barrier. Nat. Protoc. *5*, 1265–1272.

Bottenstein, J. (1985). Cell Culture in the Neurosciences (Springer US).

Brewer, G.J., Torricelli, J.R., Evege, E.K., and Price, P.J. (1993). Optimized survival of hippocampal neurons in B27-supplemented neurobasal™, a new serum-free medium combination. J. Neurosci. Res. *35*, 567–576.

Canfield, S.G., Stebbins, M.J., Morales, B.S., Asai, S.W., Vatine, G.D., Svendsen, C.N., Palecek, S.P., and Shusta, E.V. (2017). An isogenic blood-brain barrier model comprising brain endothelial cells, astrocytes and neurons derived from human induced pluripotent stem cells. J. Neurochem. *140*, 874–888.

Helms, H.C., Abbott, N.J., Burek, M., Cecchelli, R., Couraud, P.-O., Deli, M.A., Förster, C., Galla, H.J., Romero, I.A., Shusta, E.V., et al. (2016). In vitro models of the blood-brain barrier: an overview of commonly used brain endothelial cell culture models and guidelines for their use. J. Cereb. Blood Flow Metab. *36*, 862–890.

Hollmann, E.K., Bailey, A.K., Potharazu, A.V., Neely, M.D., Bowman, A.B., and Lippmann, E.S. (2017). Accelerated differentiation of human induced pluripotent stem cells to blood-brain barrier endothelial cells. Fluids Barriers CNS *14*, 9.

Huber, J.D., Witt, K.A., Hom, S., Egleton, R.D., Mark, K.S., and Davis, T.P. (2001). Inflammatory pain alters blood-brain barrier permeability and tight junctional protein expression. Am. J. Physiol. Heart Circ. Physiol. *280*, H1241–H1248.

Kumar, K.K., Lowe, E.W., Jr., Aboud, A.A., Neely, M.D., Redha, R., Bauer, J.A., Odak, M., Weaver, C.D., Meiler, J., Aschner, M., et al. (2014). Cellular manganese content is developmentally regulated in human dopaminergic neurons. Sci. Rep. *4*, 6801.

Lim, R.G., Quan, C., Reyes-Ortiz, A.M., Lutz, S.E., Kedaigle, A.J., Gipson, T.A., Wu, J., Vatine, G.D., Stocksdale, J., Casale, M.S., et al. (2017). Huntington's disease iPSC-derived brain microvascular endothelial cells reveal WNT-mediated angiogenic and blood-brain barrier deficits. Cell Rep. *19*, 1365–1377.

Lippmann, E.S., Azarin, S.M., Kay, J.E., Nessler, R.A., Wilson, H.K., Al-Ahmad, A., Palecek, S.P., and Shusta, E.V. (2012). Derivation of blood-brain barrier endothelial cells from human pluripotent stem cells. Nat. Biotechnol. *30*, 783–791.

Lippmann, E.S., Al-Ahmad, A., Azarin, S.M., Palecek, S.P., and Shusta, E.V. (2014a). A retinoic acid-enhanced, multicellular human blood-brain barrier model derived from stem cell sources. Sci. Rep. *4*, 4160.

Lippmann, E.S., Estevez-Silva, M.C., and Ashton, R.S. (2014b). Defined human pluripotent stem cell culture enables highly efficient neuroepithelium derivation without small molecule inhibitors. Stem Cells *32*, 1032–1042.

Mannello, F., and Tonti, G.A. (2007). Concise review: no breakthroughs for human mesenchymal and embryonic stem cell culture: conditioned medium, feeder layer, or feeder-free; medium with fetal calf serum, human serum, or enriched plasma; serum-free, serum replacement nonconditioned medium, or ad hoc formula? All That Glitters Is Not Gold!. Stem Cells *25*, 1603–1609.

Mantle, J.L., Min, L., and Lee, K.H. (2016). Minimum transendothelial electrical resistance thresholds for the study of small and large molecule drug transport in a human in vitro blood-brain barrier model. Mol. Pharm. *13*, 4191–4198.

Obermeier, B., Daneman, R., and Ransohoff, R.M. (2013). Development, maintenance and disruption of the blood-brain barrier. Nat. Med. *19*, 1584–1596.

Qian, T., Maguire, S.E., Canfield, S.G., Bao, X., Olson, W.R., Shusta, E.V., and Palecek, S.P. (2017). Directed differentiation of human pluripotent stem cells to blood-brain barrier endothelial cells. Sci. Adv. *3*, e1701679.

Salvador, E., Shityakov, S., and Förster, C. (2014). Glucocorticoids and endothelial cell barrier function. Cell Tissue Res. *355*, 597–605.

Smith, Q.R., and Rapoport, S.I. (1986). Cerebrovascular permeability coefficients to sodium, potassium, and chloride. J. Neurochem. *46*, 1732–1742.

Stebbins, M.J., Lippmann, E.S., Faubion, M.G., Daneman, R., Palecek, S.P., and Shusta, E.V. (2017). Activation of RARα, RARγ, or RXRα increases barrier tightness in human induced pluripotent stem cell-derived brain endothelial cells. Biotechnol. J. *13*, 1700093.

Syvänen, S., Lindhe, Ö., Palner, M., Kornum, B.R., Rahman, O., Långström, B., Knudsen, G.M., and Hammarlund-Udenaes, M. (2009). Species differences in blood-brain barrier transport of three positron emission tomography radioligands with emphasis on P-glycoprotein transport. Drug Metab. Dispos. *37*, 635–643.

Tidball, A.M., Neely, M.D., Chamberlin, R., Aboud, A.A., Kumar, K.K., Han, B., Bryan, M.R., Aschner, M., Ess, K.C., and Bowman, A.B. (2016). Genomic instability associated with p53 knockdown in the generation of Huntington's disease human induced pluripotent stem cells. PLoS One *11*, e0150372.

Vatine, G.D., Al-Ahmad, A., Barriga, B.K., Svendsen, S., Salim, A., Garcia, L., Garcia, V.J., Ho, R., Yucer, N., Qian, T., et al. (2017). Modeling psychomotor retardation using iPSCs from MCT8-deficient patients

indicates a prominent role for the blood-brain barrier. Cell Stem Cell *20*, 831–843.e5.

Weksler, B.B., Subileau, E.A., Perrière, N., Charneau, P., Holloway, K., Leveque, M., Tricoire-Leignel, H., Nicotra, A., Bourdoulous, S., Turowski, P., et al. (2005). Blood-brain barrier-specific properties of a human adult brain endothelial cell line. FASEB J. *19*, 1872–1874.

Wilson, H.K., Canfield, S.G., Hjortness, M.K., Palecek, S.P., and Shusta, E.V. (2015). Exploring the effects of cell seeding density on the differentiation of human pluripotent stem cells to brain microvascular endothelial cells. Fluids Barriers CNS *12*, 13.

Zlokovic, B.V. (2008). The blood-brain barrier in health and chronic neurodegenerative disorders. Neuron *57*, 178–201.